Use of Particle Methods for Understanding Hypersonic Shock Boundary Layer Interactions

Ozgur Tumuklu[1,a)], Dr. Deborah A. Levin[1,b)] and Vassilios Theofilis[2,c)]

[1]*Department of Aerospace Engineering, 104 S. Wright St, University of Illinois Urbana-Champaign, IL 61801, USA*
[2]*School of Engineering, University of Liverpool, Liverpool L69 3GH, UK*

[a)]tumuklu2@illinois.edu
[b)]deblevin@illinois.edu
[c)]V.Theofilis@liverpool.ac.uk

Abstract. The study of laminar, shock boundary layer interactions is performed using direct simulation Monte Carlo and linear stability theory for Edney type IV flows over a double wedge and a double cone. The high-fidelity time accurate simulations are shown to characterize the complex shock interactions of such flows as well as their unsteadiness. Comparison of bow shock oscillations and Kelvin-Helmholtz instabilities are found to be consistent with earlier values in the literature.

INTRODUCTION

Strong shock interactions are complex with a number of features known as separation and reattachment shocks, the triple point, shear layers and boundary layer interactions [1]. Usually the Reynolds number that is required to study *laminar* shock interactions is sufficiently high that the application of particle, kinetic approaches such as direct simulation Monte Carlo (DSMC) or Bhatnagar Gross Krook (BGK) is too prohibitive. However, with the advent of petascale computing and improved algorithms, particle methods are able to access flow regimes where hypersonic unsteady and transitional (in the sense of laminar to turbulent) behavior occurs. Portions of this paper were presented in a special session on high Reynolds number flows organized by the second author. In particular, we consider here a summary of results presented that involve the characterization of unsteady Edney type IV flows over double cone and double wedge configurations. In both cases, when an attached shock from the first cone or wedge surface interacts with the detached bow shock from the second geometry, spatial regions with both sub- and supersonic flow in various degrees of thermochemical non-equilibrium and multiple length scales occurs. Therefore, an accurate modeling of such flows requires a kinetic consideration. In this work, numerical analyses of shock wave boundary layer interactions (SWBLI) were performed using the DSMC method, a stochastic approach to solving the Boltzmann equation.

The question arises as to why DSMC or related particle approaches should be used instead of the Navier Stokes (NS) equations. The latter approach is questionable due to rarefaction effects especially near the leading edge of slender bodies where temperature jump and the slip velocity are significant (see for example, Fig. 15 of Ref. [2]). In addition, time accuracy may be lost using implicit time integration methods whereas explicit time integration for NS solutions requires a large number of iterations. In contrast, the DSMC method is time accurate and the time step is chosen based on the local collision frequency and is not related to the numerical stability of the method. Finally, as is well known, molecular-based DSMC enables the highest fidelity treatment of thermochemical nonequilibrium in shocks and gas viscosity and conductivity. It is worth noting that the use of DSMC to model SWBLis was accomplished by Moss and Bird [3] who obtained good agreement with the heat flux data of Holden *et al* [4] for flow over a double cone. However, at that time, they could not simulate higher Reynolds number flows, only steady state solutions were obtained, and there was no attempt to relate the DSMC flow macroparameters to stability theory. Our work aims to the study the effects of thermochemical non-equilibrium different gas species on the temporal characteristics of such flows and the role of Reynolds number and chemical reactions on the flow unsteadiness. The results presented in this paper do not include cases where chemical reactions have been modeled. Examples of such may be found in Ref. [5].

TABLE 1. Free Stream Conditions for Three Cases[a]

Freestream Parameters:	Double Wedge Experimental (2-D)	Double Wedge Degraded (2-D)	Double Cone (Axisymmetric)
Mach number	7.14	7.14	15.88
Translational temperature, K	710	710	42.6
Rotational temperature, K	710	710	42.6
Vibrational temperature, K	710	710	1986
Static pressure, kPa	0.78	0.098	0.0022
Velocity, m/s	3812	3812	2073
Density, kg/m^3	0.0037	0.000465	0.000176
Number density, molec/m^3	7.96×10^{22}	1.0×10^{22}	3.779×10^{21}
Stagnation enthalpy, MJ/kg	8.0	8.0	2.2
Unit Reynolds number, 1/m	4.15×10^{5}	5.22×10^{4}	9.35×10^{4}
Mean free path, m	2.05×10^{-5}	1.64×10^{-4}	2.17×10^{-4}
Knudsen number	4.08×10^{-4}	3.24×10^{-3}	1.89×10^{-3}

[a]Running gas is nitrogen.

DSMC NUMERICAL PARAMETERS AND PHYSICAL MODELS

The Statistical Modeling In Low-density Environment (SMILE) [6] computational solver was used in all simulations presented below. SMILE employs the majorant frequency scheme for modeling the molecular collision frequency [7], and the variable hard sphere (VHS) model for modeling the interaction between particles [8]. The discrete Larsen-Borgnakke (LB) [9] model prohibiting double relaxation [10] was used to model rotational-translational (R-T) and vibrational-translational (V-T) energy transfer. More specifically, Millikan and White (MW) [11] and Parker‘s rates [12] with the DSMC correction factors [13, 14] were used to model (V-T) and (R-T) relaxation rates, respectively. As mentioned earlier, for the examples shown in this paper, chemical reactions were not modeled. However, reacting air cases have been considered and are described elsewhere [5] using the total collision energy (TCE) approach [8]. Gas-surface interactions were modeled using the Maxwell model with full momentum and energy accommodation.

As shown in Table 1, the conditions for the three cases that are considered in this paper are near-continuum. Therefore, we carefully considered the convergence of DSMC numerical parameters to ensure that they did not impact the results. The conventional DSMC numerical requirements are that the number of computational particles per volume with a linear size equal to the local gas mean free path, λ, is on the order of three, the time step is such that simulated particles do not cross more than one cell during a single time step, and the collision cell size should be less than the local mean free path. To satisfy the DSMC cell size requirement, the SMILE code employs a two level Cartesian grid, namely a coarse level and refined level, in order to capture large flow gradients in the simulation domain. The coarser grid is known as the background grid in which the sampling process to calculate macro-parameters takes place. The refined, collision grid, is constructed by subdividing the background cells based on the local density gradient values, the number of particles in the cell, and a user-defined parameter which controls the maximum number of subdivisions for a given background cell. This grid adaptation algorithm guarantees that there are at least 3-4 particles for these non-reacting cases per collision cell before allowing further divisions. It should be noted that collision frequency is calculated based on the collision cell. The number of particles per collision cell is sufficient since the majorant collision frequency algorithm is used in the selection of collision pairs in this work [7]. Table 2 summarizes the DSMC numerical parameters that were employed for the simulations shown here.

LINEAR GLOBAL STABILITY ANALYSIS AND THE RESIDUALS ALGORITHM

Least-damped eigenmode properties, such as the damping rate, frequency and amplitude function, can be recovered by analyzing the signals obtained from time accurate DSMC simulations when the flow is close to the steady state solution. Near convergence, any flow quantity, $\mathbf{q} = (u, v, T_{\text{trn}}, T_{\text{rot}}, T_{\text{vib}}, P)^T$, can be represented by the linear superposition of a steady solution, $\bar{\mathbf{q}}(x, y, z)$ and a small three-dimensional deviation from the steady state, denoted as residual,

TABLE 2. DSMC Numerical Parameters

Numerical Parameters[a]:	Double Wedge Experimental	Double Wedge Degraded	Double Cone
Number of simulated particles	2.05×10^9	1.45×10^9	2.75×10^9
Total number of time-steps	950,000	350,000	100,000
Time step, s	1.0×10^{-9}	3.0×10^{-9}	4.0×10^{-8}
Total number of collision cells	4.88×10^8	9.05×10^7	5.03×10^8

[a]At the end of the simulation

$\tilde{\mathbf{q}}(x, y, z, t)$, i.e.,

$$\mathbf{q}(x, y, z, t) = \bar{\mathbf{q}}(x, y, z) + \epsilon\tilde{\mathbf{q}}(x, y, z, t) \tag{1}$$

where ϵ is assumed to be small. As discussed in Refs. [15, 16, 17], the convergence of $\mathbf{q}(x, y, z, t)$ towards $\bar{\mathbf{q}}(x, y, z)$ can be estimated by the time evolution of probes at selected local points. Based on the fact that the coefficient of the residuals is independent of time (i.e. eigenmodes decomposition discussed in Ref. [15]), three-dimensional perturbations developing upon a steady laminar two-dimensional base state can be described by a perturbation of the form:

$$\tilde{\mathbf{q}}(x, y, z, t) = \hat{\mathbf{q}}(x, y)\mathrm{e}^{\mathrm{i}[\beta z - \omega t]} + c.c. \tag{2}$$

where the wavenumber parameter, β, is defined as $2\pi/L_z$, L_z being the spanwise extent of the three-dimensional domain. The analogous Ansatz for axisymmetric geometries is $\hat{\mathbf{q}}(x, y)\exp^{i(m\phi-\omega t)}$, where $m = 0, 1, 2...$ is an integer azimuthal wavenumber parameter. In planar geometries and a temporal analysis framework [18], the β parameter is taken to be a real number whereas the eigenmodes, $\hat{\mathbf{q}}(x, y)$, and ω may be complex. In the present analysis, attention is paid to two-dimensional perturbations only, which correspond to $\beta = 0$ (or $m = 0$ as the case might be). Therefore, Equation 2 can be written in a two-dimensional context:

$$\mathbf{q}(x, y, t) = \bar{\mathbf{q}}(x, y) + \epsilon\,[\hat{\mathbf{q}}_r \mathrm{cos}\omega_\mathrm{r} t - \hat{\mathbf{q}}_i \mathrm{sin}\omega_\mathrm{r} t]\mathrm{e}^{\sigma t} \tag{3}$$

where σ=ω_i is the damping rate and can be approximated from the logarithmic derivative of the DSMC signal as:

$$\sigma \simeq \frac{d\,(\mathrm{In}[\mathbf{q}(x, y, t) - \bar{\mathbf{q}}(x, y)])}{dt} \tag{4}$$

by combining Eqs. 1 and 3 and assuming the waves are stationary ($\omega_\mathrm{r} = 0$) [19, 20]. Note, however, that the assumption of stationary modes is not inherent to the residuals algorithm approach, which has been shown to be able to recover time-periodic linear pertubations [17].

RESULTS

The time characteristics of boundary layer shock interaction flows over the aforementioned geometric configurations are studied in a time accurate fashion by means of the DSMC method. We start with the double wedge geometry for two conditions and then consider the analysis of unsteady behavior on the double cone.

DSMC study of the unsteady behavior for a double wedge geometry

The experiments on the double-wedge configuration [21] have motivated a number of recent numerical studies using continuum CFD [22, 23] and DSMC [24, 25] approaches that were part of the NATO RTO-AVT 205 program in the Assessment of Predictive Capabilities for Aerothermodynamics Heating of Hypersonic Systems [1]. In general, it was found that the numerical calculations did not agree well the measured data in time. More specifically, our DSMC heat flux predictions for the conditions corresponding to the "Double Wedge - experimental case", the first column of Table 1, were found to be in fair agreement with the data at the beginning of the simulation; however, significant differences were observed at later simulation times. Investigation of a three-dimensional model showed that the flow is truly three-dimensional and does not reach steady state during the run time of the experiment of 242 μs [24].

To understand the time dependence of the macroparameters more clearly, we examined macroparameters such pressure in the vicinity of the separation region, as shown in Figure 1(a). The separation shock is developed above

the boundary layer due to the large adverse pressure gradient to turn the flow at the hinge. The heat transfer rates computed using two-dimensional DSMC simulations for different times were compared with those obtained from the experiment and it was observed that the surface heating values at 0.1 ms are in good agreement with the experiment, especially in the region close to the tip the first wedge and at the second wedge surface, while in time the differences between the measured and calculated values become large [25]. Furthermore, the size of the separation increased between 0.1 and 0.4 ms but later the separation point moves towards the downstream direction. It should be noted that the DSMC data presented in Figure 1(a) was obtained by averaging of the particle data in the 0.002 ms time interval.

In previous work [24], the macro-parameter sampling was conducted in batches so that flow transients in the DSMC solution could be observed, but, the time evolution of the solution was found to depend on the size of the time window. In fact, the batch size should be small enough to capture the unsteadiness and large enough to reduce the statistical noise of the DSMC method. To investigate the time evolution of the temperature and the velocity values in the x- and y-directions more closely, numerical probes were placed at two critical locations, where the separation starts and ends, as shown in Figure 1(a) at locations 4 and 14. The probed data for location 4 that was obtained by sampling each timestep (1 ns) is shown in Figure 1(b). Note that the number of particles in the aforementioned locations was found to be around 70,000 which provides sufficient statistics for sampling in each timestep. As can be seen, the simulation does not reach steady state in a time interval of 1 ms. The structure of the separation region changes after 0.5 ms where the velocity values become positive again. Additionally, the pressure values (not shown) have a tendency to increase in time which may result in the relocation of the separation region.

The topology of the separation zone and the magnitude of the velocity values inside the zone provide an opportunity to identify linear global laminar separated flow instabilities. Reference [26] studied the instability properties of incompressible laminar boundary layer flows over a two-dimensional flat-plate and found that the regime with the multiple bubbles originating from the merging of separation and reattachment points is structurally unstable and can become linearly unstable through self-excitation of three-dimensional linear (exponentially amplifying) global pertubations. Additionally, if the magnitude of the reversed velocity in the separation zone reaches on the order of 10% of its value outside the zone, then a stationary three-dimensional global mode can become linearly unstable and alter the spatial characteristics of the two-dimensional laminar separation bubble. This instability scenario has been confirmed to exist in a multitude of massively separated flows, see Ref. [27] for details.

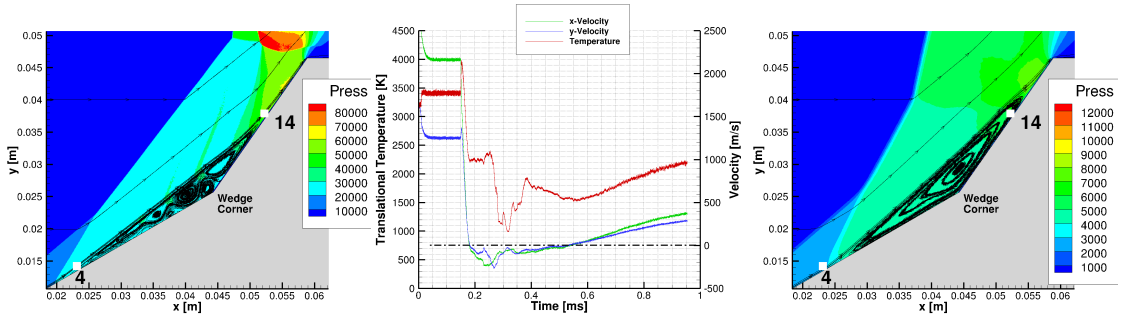

(a) Pressure at 0.8 ms, Pa.

(b) Time evolution of the flowfield parameters at location 4.

(c) Pressure in the vicinity of wedge corner.

FIGURE 1. Unsteadiness of flowfield parameters of the N_2, double wedge case for the 2-D case. First two figures and last figure represent the experimental and density degraded cases, respectively. Dashed line represents zero velocity line.

As shown in Figure 1(a), the existence of multi-structural vortices and high-velocity values in the separation region suggests that characterizing the unsteadiness of the experimental case will be difficult. Therefore, we defined a case at a lower Reynolds number than the experiment, which still exhibits similar hypersonic SBLIs by reducing the free stream number density by a factor of eight, compared to the experimental value. We refer to this case as the "density degraded case," with free stream parameters given in the second column of Table 1. Comparison of Figure 1 (a) and (c) shows that the extent of the separation region is smaller in the degraded case and the multiple bubble structure disappears. As was shown in Ref. [25], this flow does indeed come to steady state, in contrast to the experimental case, in a length of time on the order of 1 ms. Application of the window proper orthogonal decomposition (WPOD)

method[5] to analyze the modes that bring this flow to steady state have shown that the spatial part of the first mode for each flow quantity approximately outlines the corresponding steady-state solution since the magnitude of the first temporal mode is at least an order of magnitude higher in comparison to higher modes. Higher spatial POD modes, on the other hand, are larger in magnitude in the bow, separation and transmitted shocks, and shear layers where these structures were found to be coupled to each other, similar to the behavior that will be shown below for the double cone. Research is underway to understand whether these modes are the same for a full three-dimensional DSMC simulation using the SUGAR code [28] since it is possible that the 3-D pressure relief effect may reduce the time and change the manner in which the flow reaches steady state.

DSMC and RA study of unsteady flow over the double cone geometry

The objective of these simulations was to combine for the first time the DSMC method with linear global stability analysis and momentum potential theory [29] to address the question of unsteadiness in SLBLI. The well-known sharp 25/55 degree double cone model [4] was selected as the geometry of interest with the free stream conditions for the simulations taken from [4], as given in the third column of Table 1. Detailed information about the selection of numerical parameters, numerical convergence of the DSMC simulations, as well as a description of the results obtained for the macroscopic flow quantities is discussed in Ref. [19]. The baseline condition for which measurements were obtained corresponded to a unit Reynolds number $Re = 9.35 \times 10^4$ m^{-1}, but, other cases with increased Reynolds numbers were modeled as well by increasing the free stream static pressure from 2.2, 4.4 and 8.8 Pa to get to a *high-Re* case of 3.74×10^5 m^{-1}.

An important way to study the unsteadiness in laminar SWBLI flows is to examine the spatial distribution of the amplitude function. Figure 2 shows these for the highest Reynolds number case, 3.74×10^5 m^{-1}, considered. We note that all length scales, velocities, and times are normalised with respect to the length of the first cone, $L = 0.1016$ m, a freestream velocity $U_\infty = 2073$ m s^{-1}, and the characteristic time required for the undisturbed flow to travel along the first cone, L/U_∞, respectively. Similarly, a total temperature of 1907 K and a maximum pressure of 1425 Pa for the Holden experimental $Re = 9.35 \times 10^4$ were used to normalise the temperature and pressure values. The general features that are observed are related to the axial component, $\hat{u}$, of the perturbation velocity, which is found to decrease inside the shock as well as in the separation region, whereas the opposite behavior is observed for the radial component of the velocity perturbation, $\hat{v}$. The effect of thermal nonequilibrium on the amplitude functions is also distinctive for the three temperature (translational, rotational, and vibrational) perturbation components. The amplitude function of the translational and rotational temperature perturbations, $\hat{T}_{trn}$ and $\hat{T}_{rot}$, seen in Figure 2(c) and (d) are found to have an analogous spatial structure as the velocity perturbations, which may be explained by the high relaxation rate of these two modes. In contrast, the amplitude function of the vibrational temperature, $\hat{T}_{vib}$, seen in Figure 2(e), is practically confined in its entirety within the separation region. Finally, the spatial distribution of the pressure perturbation, $\hat{P}$, seen in Figure 2(f), clearly shows the same coupling between the primary shock system and the separation zone, as well as streamwise periodic pressure perturbations on the downstream cone surface.

Most importantly are the presence of λ-shocklets, *i.e.,* the braided structure seen in between the shear and boundary layers, consistent with the change in sign change in the amplitude function. As has been shown by Duck *et al.* [30] the interactions of self-induced acoustic and thermal disturbance waves with shock waves and the hypersonic boundary layer can cause flow unsteadiness [30] and these perturbations increase as we increase the Reynolds number. The interaction of the λ-shocklets with shear layer creates acoustic disturbances that can propagate in the upstream direction and interact with the bow shock. Shock oscillations appear on the bow shock, while the amplitude functions $\hat{u}, \hat{v}, \hat{T}_{trn}, \hat{T}_{rot}$ and $\hat{P}$ also connect at the triple point shock perturbations with those in the (now substantially larger) separation zone. By contrast, $\hat{T}_{vib}$ is again confined within the separation region, although at this Reynolds number this amplitude function features additional peaks at the downstream cone wall; the latter could be interpreted as boundary layer perturbations, although resolution of the boundary layer at this Reynolds number is extremely challenging.

The DSMC double cone simulations were used in two other quantitative analyses of the flow unsteadiness. Doak's momentum theory, based on a Helmholtz decomposition of the DSMC data allowed us to separate the flow disturbances into acoustic and thermal components without assuming a priori that the disturbance is linear. Momentum potential theory showed that the vorticity striations in the bow shock at Reynolds number = 374,000 m^{-1} are an an outcome of the acoustic disturbances generated in the vicinity of the separation region and λ-shock patterns. The thermal component of the momentum density was found to be large in the shear layer but the spatial distribution of both acoustic and thermal disturbances became more uniform especially in the SWBLI region at a later time. Other Reynolds number case results may be found in Ref. [20]. This study is the first time that the Doak's momentum

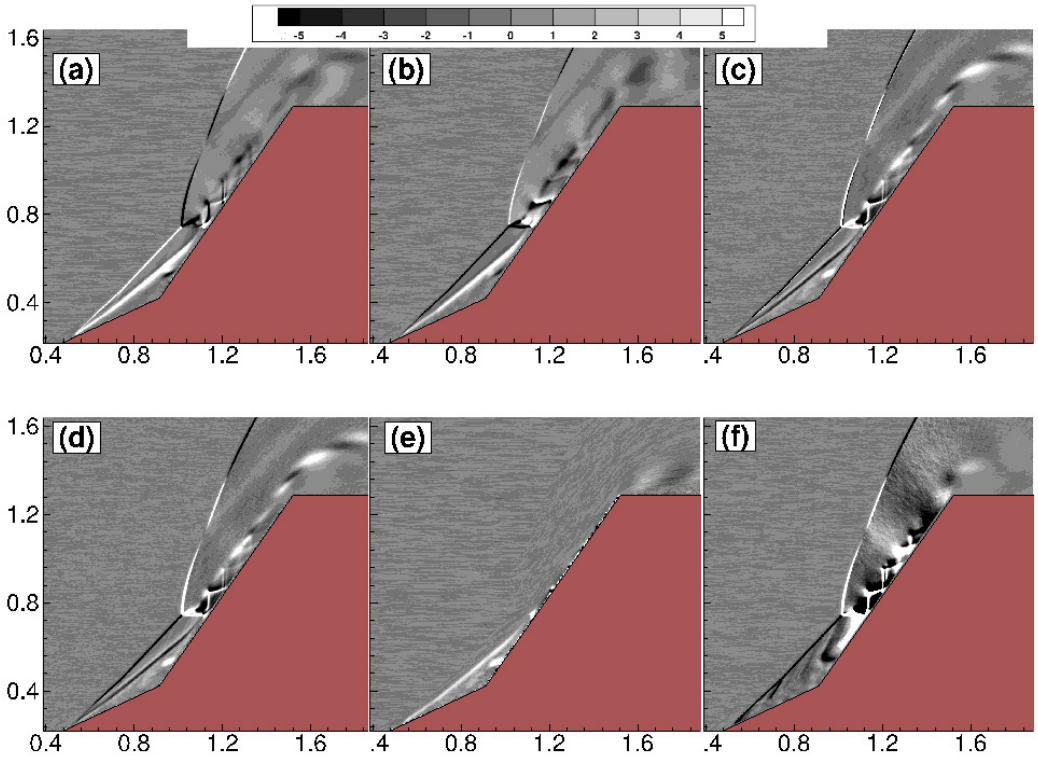

FIGURE 2. Normalised amplitude functions of least-damped linear global mode at Re=374,000 m^{-1}. (a) $\hat{u}$; (b) $\hat{v}$; (c) $\hat{T}_{\text{trn}}$; (d) $\hat{T}_{\text{rot}}$; (e) , $\hat{T}_{\text{vib}}$; (f) $\hat{P}$.

analysis has been applied to any un-stationary, laminar SWBLI flows simulated by either NS or DSMC. In addition, a fast Fourier transform of the DSMC signal in the vicinity of the shear layer near the corner of the second cone obtained dominant frequencies for a Kelvin-Helmholtz instability of 45 and 70 kHz with a convective Mach number of 0.32 - 018. These agree well with earlier experiments of Martens *et al* [31] for Strouhal numbers in the range of $0.2 \leq St \leq 0.37$ where

$$St = \frac{f\delta_W}{U_1.}$$

Furthermore, characteristic low frequencies of about 2 kHz were observed at the separation point and bow shock, consistent with the DNS simulations of Wu and Martin *et al* [32].

CONCLUSIONS

We have found that with proper consideration of DSMC numerical parameters, it is possible to model and analyze unsteady, laminar flows with strong shock interactions in a time accurate manner. The DSMC is found to resolve the wide range of length scales exhibited in these flows and with very good resolution of the shock-shock interactions. We considered here two cases, both involving Edney Type-IV interactions for flows over a double wedge and a double cone using non-reacting nitrogen as the working fluid. Linear stability analyses using the time-accurate DSMC macroparameters was able to predict a global eigenmode for the flow, proving a theoretical basis for establishing steady state as well as reducing computational expense. In the case of the double wedge, it was found that reducing the free stream Reynolds number by about an order of magnitude from the original measurement allowed us to model in a fully time-accurate manner, a flow which comes to steady state. The axial symmetry of the well known double cone geometry has allowed us consider higher Reynolds numbers wherein, the flow remains laminar, however, the presence of λ-shocklets and a Kelvin-Helmholtz instability suggest that this case is one that approaches transition.

More work is clearly needed but the future is promising. One can envision the use of advanced chemistry and gas-surface models which can be naturally implemented in DSMC will have an important effect on the flow stability. In future work, we seek to understand more clearly these effects as well as the effect of three-dimensionality on the flow stability.

ACKNOWLEDGMENTS

The research of OT and DL was supported by the Air Force Office of Scientific Research through AFOSR Grant No. FA9550-11-1-0129 with a subcontract award number 2010-06171-01 to UIUC. OT and DL are also grateful for the computational resource provided on ERDC Topaz, AFRL Spirit and Thunder. The work of VT is sponsored by the Air Force Office of Scientific Research, Air Force Material Command, USAF, under Grant No. FA9550-15-1-0387 *Global transient growth mechanisms in high-speed flows with application to the elliptic cone*, with VT as Principal Investigator and Dr. Ivett Leyva as Program Officer.

REFERENCES

[1] D. Knight, O. Chazot, J. Austin, M. A. Badr, G. Candler, B. Celik, D. de Rosa, R. Donelli, J. Komives, A. Lani, D. Levin, I. Nompelis, M. Panesi, G. Pezzella, B. Reimann, O. Tumuklu, and K. Yuceil, Progress in Aerospace Sciences **90**, 39 – 53 (2017).

[2] O. Tumuklu, Z. Li, and D. A. Levin, AIAA Journal **54**, 3701–3716 (2016).

[3] J. N. Moss and G. A. Bird, AIAA Journal **43**, 2565–2573 (2005).

[4] M. S. Holden, T. P. Wadhams, G. V. Candler, and J. K. Harvey, AIAA Paper **1131**, p. 2003 (2003).

[5] O. Tumuklu, D. Levin, and V. Theofilis, Accepted for publication in Physical Review Fluids (2019).

[6] M. S. Ivanov, G. N. Markelov, and S. G. Gimelshein, "Statistical simulation of reactive rarefied flows - numerical approach and applications," AIAA paper 1998-2669, AIAA/ASME Joint Thermophysics and Heat Transfer Conference, 7th, Albuquerque, NM, June 15-18 (1998).

[7] M. S. Ivanov and S. V. Rogasinsky, Soviet Journal of Numerical Analysis and Mathematical Modeling **3**, 453–465 (1988).

[8] G. A. Bird, in *Molecular Gas Dynamics and the Direct Simulation of Gas Flows* (Clarendon, Oxford, England, U.K., 1994).

[9] P. S. Larsen and C. Borgnakke, Journal of Computational Physics **18**, 405–420 (1975).

[10] B. L. Haas, D. Hash, G. A. Bird, F. E. Lumpkin, and H. Hassan, Physics of Fluids A **6**, 2191–2201 (1994).

[11] R. C. Millikan and D. R. White, Journal of Chemical Physics **39**, 3209–3213 (1963).

[12] J. G. Parker, Physics of Fluids **2**, 449–462 (1959).

[13] F. E. Lumpkin, B. L. Haas, and I. D. Boyd, Physics of Fluids A: Fluid Dynamics (1989-1993) **3**, 2282–2284 (1991).

[14] N. E. Gimelshein, S. F. Gimelshein, and D. A. Levin, Physics of Fluids **14**, 4452–4455 (2002).

[15] V. Theofilis, "On steady–state flow solutions and their nonparallel global linear instability," in 8^{th} *European Turbulence Conference, June 27–30, 2000*, edited by C. Dopazo (Barcelona, Spain, 2000), pp. 35–38.

[16] V. Theofilis and T. Colonius, "An algorithm for the recovery of 2- and 3-d biglobal instabilities of compressible flow over 2-d open cavities," in *33 rd AIAA Fluid Dynamics Conference and Exhibit* (2003).

[17] F. Gomez, S. Le Clainche, P. Paredes, M. Hermanns, and V. Theofilis, AIAA Journal **50**, 2731–2743 (2012).

[18] V. Theofilis, Annual Review of Fluid Mechanics **43**, 319–352 (2011).

[19] O. Tumuklu, D. A. Levin, and V. Theofilis, Physics of Fluids **30**, p. 046103 (2018).

[20] O. Tumuklu, V. Theofilis, and D. Levin, Physics of Fluids **30** (2018).

[21] A. Swantek and J. Austin, AIAA Journal **53**, 311–320 (2014).

[22] M. Badr and D. Knight, "Shock wave laminar boundary layer interaction over a double wedge in a high mach number flow," AIAA Paper 2014-1136, 52nd Aerospace Sciences Meeting, AIAA SciTech, 13-17 January 2014, National Harbor, Maryland (2014).

[23] J. R. Komives, I. Nompelis, and G. V. Candler, "Numerical investigation of unsteady heat transfer on a double wedge geometry in hypersonic flows," AIAA Paper 2014-2354, 44th AIAA Fluid Dynamics Conference, AIAA Aviation, 16-20 June 2014, Atlanta, GA (2014).

[24] O. Tumuklu, D. A. Levin, S. F. Gimelshein, and J. M. Austin, "Modeling of near-continuum laminar boundary layer shocks using DSMC," in *30th International Symposium On Rarefied Gas Dynamics: RGD30*, Vol. 1786 (AIP Publishing, 2016) p. 050004.
[25] O. Tumuklu, D. A. Levin, and V. Theofilis, "On the temporal evolution in laminar separated boundary layer shock-interaction flows using DSMC," AIAA Paper 2017-1614 (2017).
[26] V. Theofilis, S. Hein, and U. Dallmann, Philosophical Transactions of the Royal Society of London A: Mathematical, Physical and Engineering Sciences **358**, 3229–3246 (2000).
[27] W. He, R. S. Gioria, J. M. Pérez, and V. Theofilis, Journal of Fluid Mechanics **811**, 701–741 (2017).
[28] S. S. Sawant, O. Tumuklu, R. Jambunathan, and D. A. Levin, Computers & Fluids **170**, 197 – 212 (2018).
[29] P. Doak, J. Sound Vib. **131**, 67–90 (1989).
[30] P. W. Duck, D. G. Lasseigne, and M. Y. Hussaini, Theoretical and Computational Fluid Dynamics **7**, 119–139Feb (1995).
[31] S. Martens, K. W. Kinzie, and D. K. McLaughlin, AIAA J. **32**, 1633–1639 (1994).
[32] M. Wu and M. P. Martin, J. Fluid Mech. **594**, 71–83 (2008).